RESEARCH ARTICLE

Analysis of Genomewide DNA Methylation Reveals Differences in DNA Methylation Levels between Dormant and Naturally as well as Artificially Potentiated Pedicle Periosteum of Sika Deer (Cervus nippon)



CHUN YANG^{1,2}, XIAO LU^{1,2}, HONGMEI SUN^{1,2}, WEN HUI CHU^{1,2}, AND CHUNYI LI^{1,2}*

¹Institute of Special Wild Economic Animals and Plants, Chinese Academy of Agricultural Sciences, Changchun, People's Republic of China

ABSTRACT

Deer antlers are the only mammalian appendages that can fully regenerate each year from the permanent bony protuberances of the frontal bones, called pedicles. Pedicle periosteum (PP) is the key tissue for antler regeneration and the source of antler stem cells. The distal one third of the PP has acquired the ability to regenerate antlers and is termed the potentiated PP (PPP), whereas the proximal two thirds of the PP requires further interactions within its niche to launch antler regeneration and is termed the dormant PP (DPP). However, the molecular mechanisms underlying the process of potentiation from the DPP to the PPP are unknown. In this study, we used the fluorescence-labeled methylation-sensitive amplified polymorphism method to assess the levels of DNA methylation in both cells and tissues of the PPP and the DPP. The results showed that the levels of DNA methylation were significantly lower in the PPP compared to the DPP (P < 0.05). Therefore, DNA demethylation may be involved in the process of this potentiation. This involvement was further confirmed by functional testing by artificially creating a potentiated PP (aPPP) from DPP tissue. Moreover, we identified 15 methylated fragments by the methylation sensitive amplified polymorphism method that are either unique to the PPP or the DPP, which were further confirmed by Southern blot analysis. Taken together, our data suggest that DNA demethylation is involved in the process of PP potentiation, which is a prerequisite step for the initiation of antler regeneration. These findings provide the first experimental evidence to link

Grant sponsor: National Natural Science Foundation of China; Grant number: 31402059. Conflict of interest: None.

*Correspondence to: Chunyi Li, Institute of Special Wild Economic Animals and Plants, Chinese Academy of Agricultural Sciences, 4899 Juye Street, 130112, Changchun, People's Republic of China.

E-mail: lichunyi1959@163.com

Received 5 May 2016; Revised 19 July 2016; Accepted 23 July 2016

DOI: 10.1002/jez.b.22695

Published online in Wiley Online Library (wileyonlinelibrary.com).

²State key Laboratory for Molecular Biology of Special Economic Animals, Changchun, People's Republic of China

epigenetic regulation and mammalian appendage regeneration. *J. Exp. Zool. (Mol. Dev. Evol.)* 00:1–9, 2016. © 2016 Wiley Periodicals, Inc.

J. Exp. Zool. (Mol. Dev. Evol.) 00:1–9, 2016 How to cite this article: Yang C, Lu X, Sun H, Chu WH, Li C. 2016. Analysis of genomewide DNA methylation reveals differences in DNA methylation levels between dormant and naturally as well as artificially potentiated pedicle periosteum of sika deer (*Cervus nippon*). J. Exp. Zool. (Mol. Dev. Evol.) OB:1–9.

INTRODUCTION

DNA methylation, an essential type of epigenetic modification, is crucial for the establishment and maintenance of cellular identity (Bird, 2002). The level of DNA methylation is correlated with differential gene expression among different tissue types, and there is increasing evidence that DNA methylation negatively influences gene expression during cellular proliferation (Wu and Zhang, 2010; Cedar and Bergman, 2012; Franchini et al., 2012), differentiation (Alvaro et al., 2007), genomic imprinting, and regeneration (Hirose et al., 2013; Takayama et al., 2014). For example, *sonic hedgehog* (shh) gene is hypomethylated in Xenopus tadpoles, which have the ability to regenerate missing limbs; in contrast *shh* is hypermethylated in Xenopus froglets, which are unable to regenerate lost appendages (Yakushiji et al., 2007). This finding provides evidence for the possible correlation between the level of DNA methylation and tissue/organ regeneration.

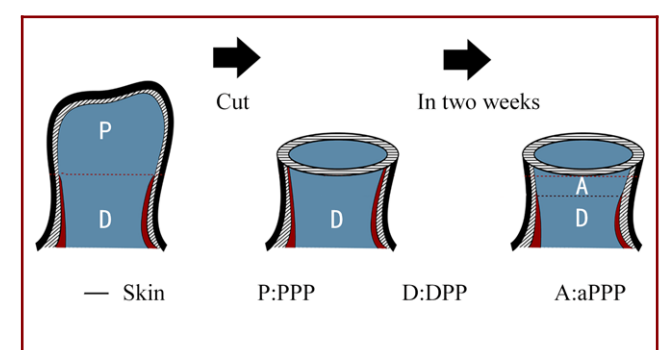
Deer antlers are unique mammalian organs in that they can fully regenerate and therefore have been used as a novel model to study regeneration of appendages/organs in mammals (Li and Suttie, 2003). Antlers regenerate from the permanent cranial bony protuberances, called pedicles. A combination of histological examination (Li et al., 2012) and tissue deletion (Li et al., 2009) convincingly demonstrated that it is the pedicle periosteum (PP), that gives rise to regenerating antlers is initiated by cells of the PP, which was first suggested by Kierdorf and Kierdorf ('92). Further studies showed that the PP cells express key embryonic stem cell markers (Oct4, Sox2, Nanog, and CD9) and could be induced to differentiate into multiple cell lineages (chondroblasts, adipocytes, myoblasts, and neuronal-like cells; Li et al., 2009). Thus, the PP cells are termed antler stem cells, and antler regeneration is considered a stem cell-based process (Li et al., 2005, 2009; Rolf et al., 2008).

While carrying out PP tissue sampling, Li and Suttie (2003) noticed that the skin of the proximal portion of a pedicle, approximately two thirds of the total pedicle length, is loosely attached to the PP; whereas the distal third of the pedicle skin was tightly bound to the PP, where antler regeneration occurs. Interestingly, antler regeneration can also take place when pedicles either naturally shorten into the proximal region as deer age, or if the distal part is artificially removed; provided that the proximal PP and the skin have already come together closely at the regeneration plane. All these observations indicate that the PP must establish interactions with the enveloping skin before

gaining the potential to regenerate antlers. To test this assumption, Li et al. (2009) carried out a functional analysis in which the pedicle skin was separated from either the distal or proximal portion of the PP by inserting an impermeable membrane, respectively. The results showed that PP of the distal pedicle stump regenerated an antler, whereas the PP of the proximal pedicle stump failed to do so after separating from the enveloping skin. Hence the distal PP is termed the potentiated PP (PPP) and the proximal PP termed the dormant PP (DPP) (Li et al., 2007). These studies demonstrated that the PP acquires the potential to regenerate an antler when it is primed via interactions with its enveloping skin, and the DPP could transform into the PPP upon becoming closely associated with skin during the annual antler regeneration process. Since antler regeneration is a complex biological process with many regulatory mechanisms involved, we hypothesise that DNA methylation is likely to be one of these mechanisms.

Methylation-sensitive amplified polymorphism (MSAP), a modification of the amplification fragment length polymorphism technique, depends on utilizing two different DNA methylation-sensitive restriction isoschizomers for the same restriction site (CCGG) (Reyna-Lopez et al., '97). MSAP has been widely used to detect genomewide differentially methylated CCGG sites, especially those from nonmodel organisms, which lack detailed genome information (Herrera and Bazaga, 2010). Fluorescence-labeled methylation-sensitive amplified polymorphism (F-MSAP), an improvement of MSAP, is based on fluorescently labeled primers and capillary gel electrophoresis with an internal lane size standard instead of traditional denaturing acrylamide gel electrophoresis and silver staining (Huang and Sun, '99). This method has been proven to be more sensitive, safer, and more effective than MSAP (Zhao et al., 2015).

The purpose of this study was to assess the relationship between the level of DNA methylation and antler stem cell potentiation from the dormant state, via comparative analysis of the genomewide DNA methylation in the PPP and the DPP. We did this at the levels of both tissues and cells of the PPP and the DPP using F-MSAP. Furthermore, we artificially created the PPP (aPPP) from the DPP state to confirm whether the correlation between level of the genomicwide DNA methylation and the PP potentiation was causally related or casually associated. Moreover, we isolated, sequenced, and identified some of the tissue-specific fragments that were differentially methylated in the PPP



Creation of artificially potentiated pedicle periosteum (aPPP)

Figure 1. Procedure for artificial creation of potentiated pedicle periosteum (aPPP) prior to the initiation of antler regeneration, the distal part (about one-third in length) of a pedicle stump was surgically removed through the junction between potentiated and dormant regions. The aPPP was then sampled at the time when the very distal edge of the enveloping pedicle skin of the dormant region became closely abutted to the distal PP and was transformed into shiny velvet-like skin 2 weeks after the operation. P: potentiated PP; D: dormant PP; A: aPPP.

over the DPP. Overall, our work provides new insights into how DNA methylation functions during the process of antler stem cell potentiation, hence antler regeneration, which is the only case of full regeneration in mammalian organs.

MATERIALS AND METHODS

Tissue Sampling and Cell Culture

The PPP and the DPP were collected from the pedicles of three 2-year-old male sika deer *(Cervus nippon)* immediately after anesthetizing in June as described by Li and Suttie (2003). The detailed protocol for the culture of the PPPc (PPP cells) and DPPc (DPP cells) were described by Li (2012). All reagents were purchased from Invitrogen for primary culture of the PPP and DPP cells.

Artificial Creation of Potentiated PP (aPPP)

An aPPP was artificially created by surgically removing the distal part of a pedicle through the junction between the potentiated and dormant regions following the procedure reported by Li et al (2007). The aPPP was then sampled at the time when the very distal edge of the enveloping pedicle skin of the dormant region became closely abutted to the distal PP and was transformed into shiny velvet-like skin 2 weeks after the operation (Fig. 1).

Genomic DNA Preparation

DNA extraction from cell culture and tissue samples of the PPP, DPP, or aPPP was carried out using a DNeasy Blood & Tissue Kit

Table 1. Sequences of adapters and primers used in F-MSAP				
Adapters/primers	Sequence (5'-3')			
EcoRI adapter	5'-CTCGTAGACTCGTACC-3'			
	3'-CATCTGACGCATGGTTAA-5'			
Hpall and Mspl adapter	5'-GACGATGAGTCTAGAA-3'			
	3'-CTACTCAGATCTTGC-5'			
E+1 primers (PreAmp)	5'-GACTGCGTACCAATTC+A-3'			
HM+1 primers (PreAmp)	5'-GATGAGTCTAGAA1CGG+T-3'			
E+3 primers	5'-GACTGCGTACCAATTC+AAC-3'			
	5'-GACTGCGTACCAATTC+AAG-3'			
	5'-GACTGCGTACCAATTC+ACA-3'			
	5'-GACTGCGTACCAATTC+AGT-3'			
	5'-GACTGCGTACCAATTC+ACT-3'			
	5'-GACTGCGTACCAATTC+AGA-3'			
	5'-GACTGCGTACCAATTC+ATG-3'			
	5'-GACTGCGTACCAATTC+ATC-3'			
HM+3 primers	5′-FAM²-GATGAGTCTAGAACGG+TAC-3′			
	5'-FAM-GATGAGTCTAGAACGG+TAG-3'			

according to the manufacturer's protocols. Extracted genomic DNA samples were dissolved in TE buffer and stored at -20° C until use.

F-MSAP Assay

The isoschizomers restriction enzymes HpaII and MspI recognize the same restriction site (5′-CCGG-3′), but have different sensitivities to methylation of the cytosine residues. The HpaII does not cleave if either of the cytosine residues is fully methylated (both strands), whereas MspI does not cleave if the external cytosine is fully methylated or hemimethylated (one strand). Thus, the differentially methylated status at the cytosine residues of CCGG sites would be recognized differently by these two different enzymes (McClelland et al., '94).

In the F-MSAP technique, the different methylation-sensitive isoschizomers (HpaII and MspI) with an internal control restriction enzyme (EcoRI) were used for DNA digestion. The enzymatically digested products were then ligated to adaptors, and preamplification and selective amplification with fluorescent-labeled primers were performed. The amplified products were checked using denaturing gel electrophoresis and sequenced by an ABI 3730xl DNA sequencer. Only the clear and reproducible bands that appeared in three runs of independent PCR amplification were scored. The F-MSAP data were analyzed using Genescan3.1 software. The adaptors and primers used in the present study were designed according to Yang et al. (2011) with minor modifications (Table 1). The detailed procedure was as follows.

DNA Digestion and Ligation

The genomic DNA from each sample was digested with EcoRI/HpaII or EcoRI/MspI, and each resultant DNA fragment

was ligated to adapters at 16°C overnight. The digestion-ligation of each sample was performed in 25 μ L solution containing 500 ng DNA template, 3 U EcoRI, 3 U HpaII (or MspI), 1.5 U T4 DNA ligase, 5 pmol EcoRI adapter, 50 pmol HpaII/MspI adapter, and 2.5 μ L 10×T4 ligase buffer. The mixture was incubated at 37°C overnight and stored at –20°C.

Preamplification PCR

Preamplification PCR was performed in 20 μ L solution containing 2 μ L of ligation products, 40 ng of E+1 and H-M+1 preamplified primers (Table 1), 0.1 μ L of Ex Taq polymerase, 1.6 μ L of dNTPs (2.5 mM), 1.2 μ L of MgCl₂ (25 mM), 2 μ L of 10× PCR buffer, and 14.1 μ L of water. The PCR conditions were as follows: 94°C for 5 min; 30 cycles of 94°C for 30 sec, 56°C for 1 min, and 72°C for 1 min; and extension at 72°C for 7 min prior to selective amplification. The PCR products from the preamplification were diluted to 1–25 (v:v) with water and stored at –20°C until use.

Selective Amplification PCR

Selective amplifications were performed in 20 μ L solution containing 2 μ L of the diluted preamplification product, 10 ng of E+3 primer, 40 ng of H-M+3 primer labeled with fluorescence dye (Table 1), 0.1 μ L of Ex Taq polymerase, 1.6 μ L of dNTPs (2.5 mM), 1.2 μ L of MgCl₂ (25 mM), and 2 μ L of 10× PCR buffer. The PCR amplification reactions were performed using the touch-down cycles, and the conditions were as follows: 94°C for 5 min; 13 touch-down cycles of 94°C for 30 sec, 65°C (subsequently reduced each cycle by 0.7°C) for 30 sec and 72°C for 1 min; 23 continued cycles of 94°C for 30 sec, 56°C for 30 sec, and 72°C for 1 min; and extension at 72°C for 7 min. The Ex Taq polymerase buffers were purchased from Takara.

Selective Amplification Products Detection

An aliquot of 0.5 μ L of selectively amplified products was added to 24.5 μ L of 70% cold ethanol, which was mixed and centrifuged at 3700 rpm for 30 min at 4°C to collect the precipitate. Subsequently, LIZ500 standard and HiDi were added to the precipitate with the final volume to 8 μ L. The solution was denatured at 94°C for 10 min and loaded onto a 4% denaturing gel. Finally, the bands were analyzed using Genescan3.1 software based on the detection of fluorescent signals of different intensity and locations relative to the LIZ500 standard. Three kinds of bands were detected, and each test was repeated three times (Table 2).

Based on the differential methylation sensitivity of isoschizomers, HpaII and MspI, cleaved band patterns were divided into three types (Fig. 2): Type I, which represents both bands for HpaII and MspI digestion, indicating no-methylation or inner methylation of single-stranded DNA (to simplify the analysis, Type I bands in our study were considered as no-methylation); Type II bands, which represent bands only

Table 2. Methylation sensitivity and restriction patterns of the Hpall and Mspl isoshizomers

	E	Enzyme sensitivities			
Methylation status	Hpall	Mspl	Н	М	
ccgg <u>c</u> cgg ggccggcc	Active	Active	1	1	
<u>C</u> CGG	Active	Inactive	1	0	
GGCC C C GG	Inactive	Active	0	1	
GG C C					

H and M indicate the enzyme combination of EcoRI /HpaII and EcoRI / MspI, respectively.

1 band present; 0 band absent. Underlined cytosine is methylated.

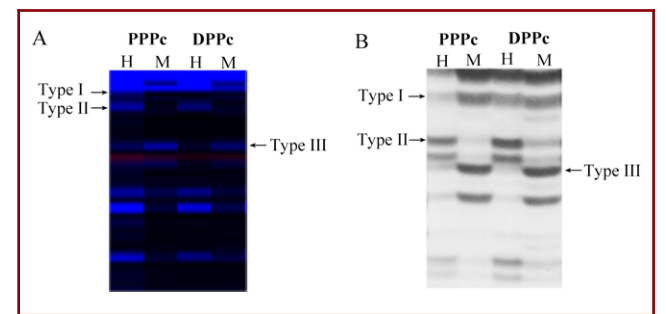


Figure 2. Cytosine methylation patterns with the primer combination H-M+TAC/E+AAC. (A) the profile from F-MSAP; (B) the profile from MSAP using silver stain; H and M refer to digestion with EcoRI/Hpall and EcoRI/Mspl; Type I, Type II, and Type III refer to unmethylated, hemimethylated and fully methylated sites, respectively.

for HpaII digestion, indicating outer methylation of a single stranded DNA and hemimethylation at the outer cytosine nucleotide in the CCGG sequence; Type III bands, which represent bands only for MspI digestion, indicating inner methylation of double-stranded DNA and full methylation of the CCGG sequence (Table 2).

The methylation ratio was calculated using the following formula:

 $\begin{aligned} \text{Methylation ratio} &= \text{Type II bands} \, + \, \text{Type III/Type I} \\ &\quad \text{[bands} \, + \, \text{Type II bands} \, + \, \text{Type III bands} \end{aligned}$

Full methylation ratio = Type III/Type I bands + Type II bands + Type III bands

Hemi methylation ratio = Type II bands/Type I bands + Type II bands + Type III bands

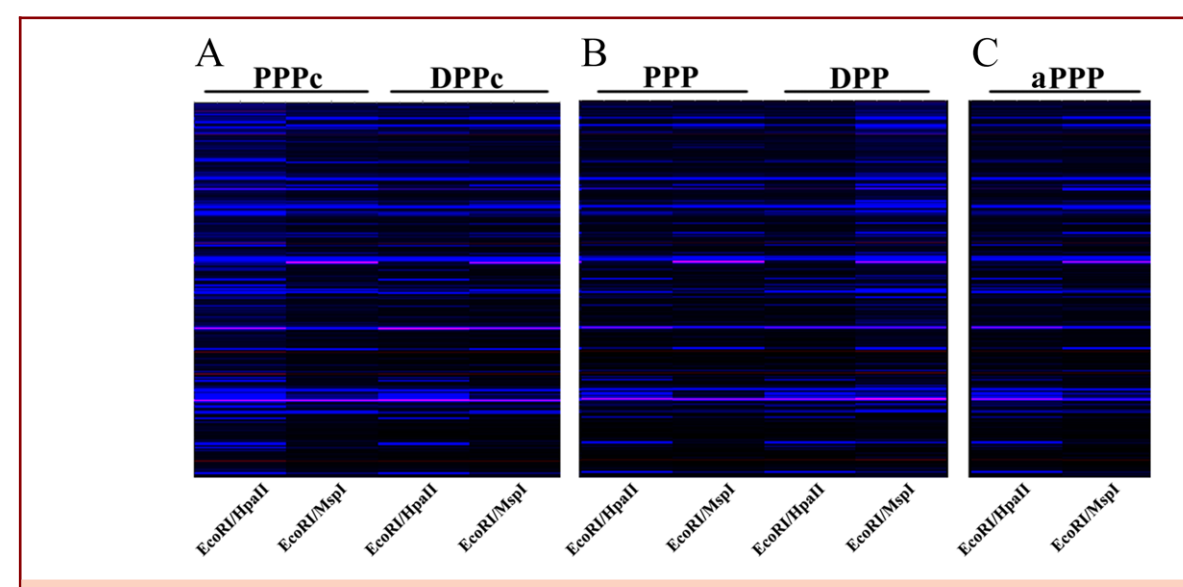


Figure 3. Methylation profiles of the cell group (PPPc and DPPc), the tissue group (PPP and DPP), and the aPPP tissue group using the combination of primers H-M+TAC/E+AAC. (A) Profile of the cell group from F-MSAP, lanes 1–2 represent PPPc and lanes 3–4 represent DPPc; (B) profile of the tissue group from F-MSAP, lanes 1–2 represent PPP and lanes 3–4 represent DPP; (C) profile of the aPPP from F-MSAP, lanes 1–2 represent aPPP.

Cloning and Sequencing of the MSAP Fragments

To isolate the MSAP fragments from the PPP and DPP, the MSAP products (see above) were denatured, separated by electrophoresis on a Long Ranger gel and stained with silver staining. Several fragments were excised directly from the wet polyacrylamide gels on the plate using a razor blade. The fragments were rehydrated with 50 µL of 95°C ddH₂O for 5 min, slowly cooled down to room temperature, and centrifuged at $12,000 \times g$ for 10 min. Supernatant of each sample was collected, and 5 μL was used as the template for reamplification. PCR reactions were performed with the same primer combinations and reaction conditions as those used in the selective amplification. After verification using a 2% agarose gel, the band was recovered using a gel extraction kit according to the manufacturer's instructions. Subsequently, the product was ligated into the vector pGM-T and transformed into E. coli strain DH5 α . The fragments were sequenced by SAN-GON. Homology search and sequence analysis were performed using the EMBL public database.

Southern Blot Analysis

Southern blot analysis was conducted to confirm the specificity of the methylation fragments. Primers were designed according to the sequence of the specific methylation fragments and were labeled with DIG to prepare for the probe. Genomic DNA (20 μ g) was digested with EcoRI-HpaII or EcoRI-MspI, and each digestion product

was electrophoresed on a 0.8% agarose gel in Tris-Borate-EDTA buffer and transferred onto Hybond-N+ membranes. Hybridization and immunological detection were carried out according to the manufacturer's protocols.

Statistical Analysis

Analysis of variance (ANOVA) and Duncan's multiple range tests were adopted for significance analysis of methylation levels among the different tissues and cells through SPSS 18.0 software. Statistical significance was set at P < 0.05. The hemimethylation ratio (%), full methylation ratio (%), and total methylation ratio (%) were calculated for each individual separately and analyzed by ANOVA, followed by Duncan's test.

RESULTS

Profiling of DNA Methylation in the PP Tissues and Cells

We used 16 pairs of selective primers labeled with fluorescent dyes to detect genomic DNA methylation status in both the PP tissues and the cells from three male sika deer. The F-MSAP gels for the cell and the tissue groups of the PPP and DPP and the tissue group of aPPP are shown in Figure 3. A total of 6088, 6006, 6030, 4704, and 4755 fragments were detected in the DPP, PPP, aPPP, DPPc, and PPPc, respectively. For each pair of primers, each individual genome displayed 98–158 fragments (Table 3).

	Cell	Cell group		Tissue group		
Types	PPPc	DPPc	aPPP	PPP	DPP	
Unmethylated bands ^a	3351	3077	3360	3336	3159	
Hemimethylated bands	552	697	1351	1334	1429	
Fully methylated bands	852	930	1319	1336	1500	
Total amplified bands ^b	4755	4704	6030	6006	6088	
Total Methylated bands ^c	1404	1627	2670	2670	2929	
Hemimethylation ratio $^{ ext{d}}$ (%) (mean \pm SD)	$11.61^{g} \pm 0.24$	$14.82^{h} \pm 0.11$	$22.40^{g} \pm 0.51$	$22.21^g \pm 0.37$	$23.49^{h} \pm 0.63$	
Full methylation ratio $^{ m e}$ (%) (mean \pm SD)	$17.92^{g} \pm 0.10$	$19.77^{h} \pm 0.15$	$21.87^{g} \pm 0.10$	$22.26^{g} \pm 0.17$	$22.26^{g} \pm 0.17$	
Methylation ratio $^{\mathrm{f}}$ (%) (mean \pm SD)	$29.53^{g}\pm0.34$	$34.59^h \pm 0.21$	$44.27^{g} \pm 0.13$	$44.47^{g} \pm 0.51$	$48.12^{h}\pm0.33$	

^aThe number of bands is the sum of 3 individuals.

DNA Methylation Levels in the PP Tissues and Cells

Three cleavage patterns were defined in this study (see the Materials and Methods section), and the results showed that the Type I methylation pattern was most frequently observed in both the tissues and the cells of the DPP and PPP, and the tissue of aPPP, which accounted for 51.88–70.47% of bands; Types II and III bands were at the similar levels and accounted for 11.61–24.62% of bands (Table 3).

ANOVA and Duncan's multiple range tests were performed to evaluate the differential methylation levels in the PP cells and tissues. As shown in Table 3, in the cell group, the methylation level was significantly decreased in the PPPc compared to that of the DPPc (P < 0.05). Consistent with this result, the methylation levels of the PPP and aPPP tissue were also significantly lower than those of the DPP (P < 0.05). These results indicate that methylation levels were significantly decreased during the transition from the dormant state (DPP) to the potentiated state (PPP), as well as the artificial PPP state. There was no significant difference in DNA methylation levels between the PPP and aPPP (P > 0.05). Overall, the methylation levels of the PPP and the aPPP were significantly lower than those of the DPP in both the PP tissues and the cells (P < 0.05).

Analysis and Confirmation of the Tissue-Specific Methylated Fragments

The tissue-specificity of methylated fragments was identified by analysis of the differential DNA methylation patterns between the PPP and the DPP. The tissue specificity of these fragments was further verified using methylation-sensitive Southern blot analysis (Fig. 4). Through comparisons with the EMBL database, 15 of these fragments were identified to have high homology with the specific regions of the genome of *Bos taurus*. Of these 15 fragments, six were located within genes, six in the 5' upstream regions, and three in the 3' downstream regions of these genes (Table 4).

DISCUSSION

In the present study, we investigated the genomewide DNA methylation during the potentiation process from the DPP to the PPP. The results showed that the methylation level of the PPP was significantly lower than that of the DPP. Likewise, the artificially created PPP (aPPP) from the DPP showed a similar low level of DNA methylation as the PPP. Our results suggest that DNA demethylation may be an important regulatory mechanism involved in antler stem cell potentiation toward antler regeneration. Furthermore, DNA demethylation may serve as an epigenetic marker for early stage antler regeneration. These findings provide the first evidence for a strong correlation between DNA methylation level and mammalian appendage regeneration.

It is accepted that DNA demethylation influences gene transcription, DNA replication, and regulation of gene expression and is generally associated with the increased level of gene expression (Goll and Bestor, 2005). For example, the demethylation of *Xenopus elongation factor 1-\alpha* in transgenic zebrafish was observed during fin regeneration (Thummel et al., 2006). During repair of damaged muscles in mammals, DNA

 $^{^{\}rm b}$ Total amplified bands = Unmethylated bands + hemimethylated bands + fully methylated bands.

 $^{{}^{}c}$ Total methylated bands = Hemimethylated bands + fully methylated bands.

^dHemimethylation Ratio = Hemimethylated bands/total amplified bands; the ratio was calculated for each individual separately and analyzed by ANOVA and Duncan's test; means with uncommon superscripts differ significantly (P < 0.05). The statistic method was same with that for fully methylation ratio and methylation ratio.

^eFully methylation ratio = Fully methylated bands/total amplified bands.

fMethylation ratio = Total methylated bands/total amplified bands.

 $^{^{\}rm g}$ The observed ratio was not significantly different (P > 0.05) from the expected ratio.

^hThe observed ratio was significantly different (P < 0.05) from the expected ratio.

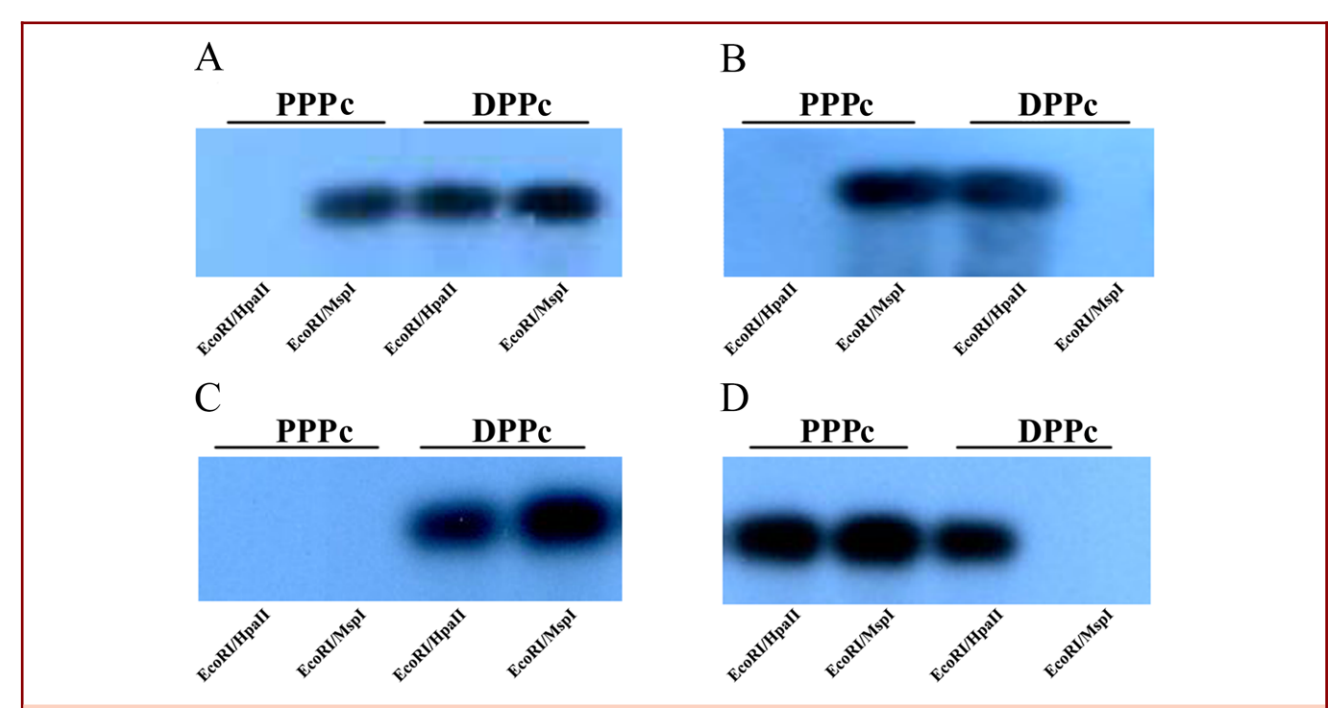


Figure 4. Confirmation of the tissue-specific methylated fragments. (A) Hybridization using probe P-2; (B) hybridization using probe P-6; (C) hybridization using probe P-27; (D) hybridization using probe P-45.

Table 4. Sequence analysis of methylated fragments					
Fragmen	nt Size (bp) (Chromosome	e Location	Gene	Identity (%)
P-2	174	1	5′side	ZPLD1	97
P-4	464	29	5′side	GAS2	98
P-5	190	11	Within	SHANK2	95
P-6	371	11	within	EHMT1	89
P-13	287	4	Within	KMT2C	98
P-15	405	29	5′side	NTM	94
P-18	205	20	5′side	NDUFS4	93
P-27	313	4	Within	RHEB	97
P-29	215	22	Within	LMCD1	86
P-30	213	23	3′side	Kcnk16	92
P-35	210	3	Within	CYP4A22	94
P-36	318	10	3′side	RAB27A	87
P-40	205	3	5′side	VWA3B	96
P-45	194	13	3′side	SNORA25	96
P-46	160	3	5′side	HIVEP3	94

demethylation of muscle progenitor cells plays a key role in the induction of reexpression of *myoD* and *myf5*, the early myogenic marker genes (Palacios and Puri, 2006). Therefore, DNA demethylation during the potentiation process of antler stem cells may be the prerequisite for this very first step of antler regeneration.

The mechanisms underlying DNA demethylation in antler stem cells are currently unknown. It is reported that DNA demethylation in general can occur through two pathways: passive and active (Bhutani et al., 2011). Passive DNA demethylation refers to the loss of the methyl group from 5-methylcytosine (5-mC) when DNA methyltransferase 1(DNMT1) is inhibited or absent during successive rounds of DNA replication (Franchini et al., 2012). Active DNA demethylation is an enzymatic process (Gadd45, MBD4, TDG, and TET) (Niehrs and Schafer, 2012) that results in the removal of the methyl group from (5-mC) by breaking a carbon–carbon bond. Activities of the enzymes involved in demethylation must be studied to reveal whether demethylation in antler stem cells during the potentiation process is achieved through passive, active, or both.

Some studies have demonstrated that some genes were characterized by their variable levels of methylation in different tissues, and under methylation in these genes in general correlated with tissue-specific gene expression (Futscher et al., 2002). In addition, it should be noted that cytosine-methylated CCGG sequences are distributed in repetitive sequences in the coding and noncoding regions that contain introns, repetitive elements, and potentially active transposable elements (Saze et al., 2011). In the present study, we found that among the 15 tissue-specific methylated fragments, six were located in the introns, six in the 5' upstream regions, and three in the 3' downstream regions of genes. The genes that contain these tissue-specific methylation

fragments may be related to tissue/organ development and regeneration, and thus constitute a core set of epimarker resource that would facilitate further epigenetic studies in antler regeneration.

Among these fragments, the one that was localized in the gene LMCD1 was only detected in the PPP. LMCD1 belongs to the LIM domain family of zinc finger proteins, and LIM proteins act as coactivators of GATA-mediated gene transcription (Rath et al., 2005). Rath et al (2005) reported that interaction between GATA6 and LMCD1 inhibits GATA6 DNA binding, resulting in repression of GATA6 transcriptional activation of downstream target genes, hence negatively impacts on lung and heart development. LMCD1 mutations have been found to promote cell migration through the Rac1-signaling pathway (Chang et al., 2012). In our studies on the transcriptome (Ba et al., in prep) and proteomes (Dong et al., 2016), we found that numerous genes related to cell migration were preferentially expressed in the PPP cells, which is considered critically important for the initiation of antler regeneration. Therefore, methylation of the LMCD1 gene might have effectively silenced the expression of the gene, hence promoted potentiation of the PP cells, i.e. the potentiated antler stem cells, to proliferate and migrate for the initiation of antler regeneration. Alternatively, gene methylation in this particular case may not have affected the status of the LMCD1 gene expression, as the methylation fragment was localized in one of the introns of the gene.

Likewise, a methylated fragment of the gene SHANK2 was also only detected in the PPP. SHANK2 is a member of the Shank family, which consists of important scaffolding proteins (SHANK1, SHANK2, and SHANK3) of postsynaptic density (Baron and Schattschneider. 2006; Grabrucker, et al., 2011). It is reported that expression of SHANK2 is mainly associated with the development of the nerve system during embryogenesis (Gessert et al., 2011). This finding seems contradictory in that when nerve growth is needed for the initiation of antler regeneration, a gene of one of the important factors associated with nerve development is methylated. However, we know that antler is a type of unusual tissue in that it only contains sensory nerves and sympathetic nerves do not grow into regenerating antler tissues from its pedicle (Li et al., '93; Suttie et al., '95). Currently, we do not know whether the Shank family stimulates/inhibits different types of nerve fibers, and if they do, methylation of the SHANK2 gene might discourage growth of sympathetic nerves into antler tissue during the stage of initial antler regeneration.

In contrast, one methylated fragment that was only localized in the gene Rheb in the DPP. Rheb is a member of the small GTPase superfamily and encodes a lipid-anchored, cell membrane protein with five repeats of the RAS-related GTP-binding region. This protein is vital in regulation of growth and cell cycle progression due to its role in the insulin/TOR/S6K signaling pathway (Heard et al., 2014). Cells of the DPP are dormant antler stem cells (Li and Chu, 2016) and must remain quiescent all the

time including during the stages of initiation of antler regeneration and growth. Therefore, methylation of the gene in the DPP might be one of the effective ways to keep the DPP in an inactive mode for the reservation of the seed cells for subsequent rounds of antler regeneration.

Antler regeneration is a complex biological process and may be controlled by many genes which are regulated by DNA methylation. In future studies, we would like to verify whether the genes that include the methylated sites found in this study are associated with antler regeneration, which will help to reveal the underlying molecular mechanisms of antler regeneration.

CONCLUSION

In this study, we found that the aPPP achieved a similar level of methylation to that of the PPP, indicating that the decrease in DNA methylation from DPP to PPP is causally related with potentiation of antler stem cells, which is the first step toward antler regeneration. Based on our present study and others, we propose that DNA methylation may be involved in regulation of regeneration-associated gene expression, although further studies are required to confirm this. Because the mechanisms underlying DNA demethylation are still not entirely understood, the process of antler stem cell potentiation may serve as a useful model for investigating this in the fast advancing epigenetic field.

ACKNOWLEDGMENTS

This research is supported by the National Natural Science Foundation of China (NO. 31402059), and Jilin province Science and Technology development plan item (NO. 20140204010YY).

LITERATURE CITED

Alvaro D, Mancino MG, Glaser S, Gaudio E, Marzioni M, Francis H, Alpini G. 2007. Proliferating cholangiocytes: a neuroendocrine compartment in the diseased liver. Gastroenterology 132:415–431.
 Baron R, Schattschneider J. 2006. The autonomic nervous system and pain. Handb Clin Neurol 81:363–382.

Bhutan N, Burns DM, Blau HM. 2011. DNA demethylation dynamics. Cell 146:866–872.

Bird A. 2002. DNA methylation patterns and epigenetic memory. Genes Dev 16:6–21.

Cedar H, Bergman Y. 2012. Programming of DNA methylation patterns. Annu Rev Biochem 81:97–117.

Chang KM, Choi SI, Kim GH. 2012. Anti-oxidant activity of *Saussurea lappa* C. B. Clarke roots. Prev Nutr Food Sci 17:306–309.

Dong Z, Wang QW, Liu Z, Sun Hongmei, Li Chunyi. 2016. Analysis of differentially expressed proteins in the potentiated and dormant antler stem cells through 2D-DIGE. Acta Vet Zootech Sin 47:92–104

Franchini DM, Schmitz KM, Petersen-Mahrt SK. 2012. 5-Methylcytosine DNA demethylation: more than losing a methyl group. Annu Rev Genet 46:419–441.

- Futscher BW, Oshiro MM, Wozniak RJ, Holtan N, Hanigan CL, Duan H, Domann FE. 2002. Role for DNA methylation in the control of cell type specific maspin expression. Nat Genet 31:175–179
- Gessert S, Schmeisser MJ, Tao S, Boeckers TM, Kuhl M. 2011. The spatio-temporal expression of ProSAP/shank family members and their interaction partner LAPSER1 during *Xenopus laevis* development. Dev Dyn 240:1528–1536.
- Goll MG, Bestor TH. 2005. Eukaryotic cytosine methyltransferases. Annu Rev Biochem 74:481–514.
- Grabrucker AM, Schmeisser MJ, Udvardi PT, Arons M, Schoen M, Woodling NS, Andreasson KI, Hor PR, Buxbaum JD, Garner CC, Boeckers TM. 2011. Amyloid beta protein-induced zinc sequestration leads to synaptic loss via dysregulation of the ProSAP2/Shank3 scaffold. Mol Neurodegener 6:65.
- Heard JJ, Fong V, Bathaie SZ, Tamanoi F. 2014. Recent progress in the study of the Rheb family GTPases. Cell Signal 26:1950–1957.
- Herrera CM, Bazaga P. 2010. Epigenetic differentiation and relationship to adaptive genetic divergence in discrete populations of the violet Viola cazorlensis. New Phytol 187:867–876.
- Hirose K, Shimoda N, Kikuchi Y. 2013. Transient reduction of 5-methylcytosine and 5-hydroxymethylcytosine is associated with active DNA demethylation during regeneration of zebrafish fin. Epigenetics 8:899–906.
- Huang JC, Sun M. 1999. A modified AFLP with fluorescence-labelled primers and automated DNA sequencer detection for efficient fingerprinting analysis in plants. Biotechnol Tech 13: 277–278.
- Kierdorf H, Kierdorf U. 1992. State of determination of the antlerogenic tissues with special reference to double-head formation. In: Brown, RD. (ed.) The biology of deer. Springer-Verlag, New York. p. 525–531.
- Li C, Chu W. 2016. The regenerating antler blastema: the derivative of stem cells resident in a pedicle stump. Front Biosci (Landmark Ed) 21:455–467.
- Li C, Harper A, Puddick J, Wang W, McMahon C. 2012. Proteomes and signalling pathways of antler stem cells. PLoS One 7:e30026.
- Li C, Sheard PW, Corson ID, Suttie JM. 1993. Pedicle and antler development following sectioning of the sensory nerves to the antlerogenic region of red deer (*Cervus elaphus*). J Exp Zool 267: 188–197.
- Li C, Suttie JM. 2003. Tissue collection methods for antler research. Eur J Morphol 41:23–30.
- Li C, Suttie JM, Clark DE. 2005. Histological examination of antler regeneration in red deer (*Cervus elaphus*). Anat Rec A Discov Mol Cell Evol Biol 282:163–174.
- Li C, Yang F, Li G, Gao X, Xing X, Wei H, Deng X, Clark DE. 2007. Antler regeneration: a dependent process of stem tissue primed via interaction with its enveloping skin. J Exp Zool A Ecol Genet Physiol 307:95–105.

- Li C, Yang F, Sheppard A. 2009. Adult stem cells and mammalian epimorphic regeneration-insights from studying annual renewal of deer antlers. Curr Stem Cell Res Ther 4:237–25.
- McClelland M, Nelson M, Raschke E. 1994. Effect of site-specific modification on restriction endonucleases and DNA modification methyltransferases. Nucleic Acids Res 22:3640–3659.
- Niehrs C, Schafer A. 2012. Active DNA demethylation by Gadd45 and DNA repair. Trends Cell Biol 22:220–227.
- Palacios D, Puri PL. 2006. The epigenetic network regulating muscle development and regeneration. J Cell Physiol 207:1–11.
- Rath N, Wang Z, Lu MM, Morrisey EE. 2005. LMCD1/Dyxin is a novel transcriptional cofactor that restricts GATA6 function by inhibiting DNA binding. Mol Cell Biol 25:8864–8873.
- Reyna-Lopez GE, Simpson J, Ruiz-Herrera J. 1997. Differences in DNA methylation patterns are detectable during the dimorphic transition of fungi by amplification of restriction polymorphisms. Mol Gen Genet 253:703–710.
- Rolf HJ, Kierdorf U, Kierdorf H, Schulz J, Seymour N, Schliephake H, Napp J, Niebert S, Wolfel H, Wiese KG. 2008. Localization and characterization of STRO-1 cells in the deer pedicle and regenerating antler. PLoS One 3:e2064.
- Saze H, Kakutani T. 2011. Differentiation of epigenetic modifications between transposons and genes. Curr Opin Plant Biol 14:81–87
- Suttie JM, Li C, Sheard PW, Corson ID, Waldrup KA. 1995. Effects of unilateral cranial sympathectomy either alone or with sensory nerve sectioning on pedicle growth in red deer (*Cervus elaphus*). J Exp Zool 271:131–138.
- Takayama K, Shimoda N, Takanaga S, Hozumi S, Kikuchi Y. 2014. Expression patterns of dnmt3aa, dnmt3ab, and dnmt4 during development and fin regeneration in zebrafish. Gene Expr Patterns 14:105–110.
- Thummel R, Burket CT, Hyde DR. 2006. Two different transgenes to study gene silencing and re-expression during zebrafish caudal fin and retinal regeneration. ScientificWorldJournal 6(Suppl 1):65–81.
- Wu SC, Zhang Y. 2010. Active DNA demethylation: many roads lead to Rome. Nat Rev Mol Cell Biol 11:607–620.
- Yakushiji N, Suzuki M, Satoh A, Sagai T, Shiroishi T, Kobayashi H, Sasaki H, Ide H, Tamura K. 2007. Correlation between Shh expression and DNA methylation status of the limb-specific Shh enhancer region during limb regeneration in amphibians. Dev Biol 312:171–182.
- Yang C, Zhang M, Niu W, Yang R, Zhang Y, Qiu Z, Sun B, Zhao Z. 2011. Analysis of DNA methylation in various swine tissues. PLoS One 6:e16229.
- Zhao Y, Chen M, Storey KB, Sun L, Yang H. 2015. DNA methylation levels analysis in four tissues of sea cucumber *Apostichopus japonicus* based on fluorescence-labeled methylation-sensitive amplified polymorphism (F-MSAP) during aestivation. Comp Biochem Physiol B Biochem Mol Biol 181:26–32.